Energy Conversion and Management: X 3 (2019) 100014

Contents lists available at ScienceDirect

Energy Conversion and Management: X

journal homepage: www.journals.elsevier.com/energy-conversion-and-management-x

Techno-economic analysis of combined inverted Brayton – Organic Rankine cycle for high-temperature waste heat recovery

Kirill A. Abrosimov[a,*], Andrea Baccioli[b], Aldo Bischi[a]

[a] Skolkovo Institute of Science and Technology, 3, Nobelya Ulitsa, Skolkovo Innovation Centre, Moscow, Russian Federation
[b] Department of Energy, Systems, Territory and Constructions Engineering, University of Pisa, Largo Lucio Lazzarino, 56122 Pisa, Italy

ARTICLE INFO

Keywords:
Inverted Brayton cycle
Organic Rankine cycle
Waste heat recovery
High-temperature exhaust
Techno-economic analysis

ABSTRACT

Many practical cases with waste heat recovery potential such as exhaust gases of reciprocating engines, cement kilns or heat-treating furnaces, are nowadays often integrated with organic Rankine cycle to convert waste heat to the mechanical power. However, when dealing with high-temperature waste heat, organic Rankine cycle faces efficiency limit due to the physical properties of the working and thermal fluids. That gives room for further enhancement of the waste heat recovery technologies via the investigation of different non-conventional schemes as one of the possible ways. In the present work, a system introducing the combined inverted Brayton plus organic Rankine cycle is under investigation. Aspen Hysys models of both conventional organic Rankine cycle and combined cycle were designed, orienting on waste heat recovery from the heavy-load gas-fueled reciprocating engine exhaust. In this way, the performance of the combined scheme was benchmarked versus the conventional organic Rankine cycle. An assessment of the organic Rankine cycle working fluids was provided, and pentane has shown the best thermodynamic performance. The study on inverted Brayton cycle defined the remarkable effect of the water condensation in the gas duct on the inverted Brayton cycle performance. Finally, both thermodynamic and economic optimizations of the models were conducted, setting the stage for the comparison of solutions. Results have shown the 10% advantage of the combined scheme over organic Rankine cycle in generated power and system efficiency. The levelized-cost-of-energy-based optimization for variable capacity factors has highlighted above 6% advantage of the investigated solution. The analysis of the sensitivity from machines' efficiencies and heat exchangers' pinches has shown that with some sets of parameters, the studied scheme may concede to the organic Rankine cycle.

1. Introduction

The general trend of developed countries for decarbonization of economy and pollution reduction continues increasing the pressure on industry expressed in the growth of carbon dioxide (CO_2) taxation and strengthening regulations. Federal Energy Management Program in the USA [1], Climate Change Agreement in the United Kingdom [2], not to say, Paris agreement [3] set the direction of this trend and prescribe the tightening changes. This economic pressure and targeted investment became a driver for many new technical fields. One of them is waste heat recovery (WHR) for power generation and technological processes.

Reach variety of technologies for WHR was scientifically studied: steam Rankine cycle (SRC), organic Rankine cycle (ORC), organic Flash cycle (OFC), conventional and inverted Brayton cycle (IBC), supercritical and transcritical CO_2 (sCO_2 and tCO_2), Kalina cycle, Stirling cycle, Thermoelectric generators (TEG), and other solutions and their combinations, which are less studied in the scientific literature. Some of these technologies have already been applied in industrial practice. The description and analysis of the majority of WHR technologies can be found in the work of Jouhara (2018) [4]. Lecompte (2015) [5] has reviewed the recent studies of ORC, which were conducted in the last years for different areas of application, working fluids, and heat source temperatures. For the on-road engines, ORC for the WHR was observed by Lion (2017) [6]. Application of ORC for WHR from technological processes was studied by Campana (2013) [7], who estimated the potential of the large-scale realization of this technology in 20 000 GWh/year of recovered thermal energy and 7.6 Mton of non-produced CO_2. sCO_2 and tCO_2 were investigated in several works, e.g., Wang X. (2016) [8] or Marchionni (2018) [9]. Ref. [8] has compared tCO_2 and ORC for the WHR from primary sCO_2 cycle, concluding that for a range of

* Corresponding author.
E-mail address: kirill.abrosimov@skolkovotech.ru (K.A. Abrosimov).
URLs: http://www.skoltech.ru (K.A. Abrosimov), http://www.destec.unipi.it (A. Baccioli).

https://doi.org/10.1016/j.ecmx.2019.100014
Received 29 January 2019; Received in revised form 27 June 2019; Accepted 30 June 2019
Available online 06 July 2019

Nomenclature

D	diameter, m
H	enthalpy, J/kg
p	pressure, Bar
P	power, kW
$\dot{q}$	heat flow, kW
r	discount rate, %
r_v	volume ratio, –
Re	Reynolds number
v	velocity, m/s
η	efficiency, %
μ	dynamic viscosity, Pa × s
π	pressure ratio, –
π'	inverse pressure ratio, –
ρ	density, kg/m^3

Subscripts

amb	ambient
av	available
BC	refer to BC
b.c.	base conditions
BM	bare module
C	refer to the Compressor
Con	refer to the Condenser of the ORC
cond	condensation
cr	critical
evap	evaporation
Ev	refer to the Evaporator
Exp	refer to the Expander of the ORC
g	gas (exhaust gas from the primary engine)
gen	refer to generator
gross	gross parameter
IBC	refer to IBC
in	inlet
is	isentropic
net	net parameter
out	outlet
s.h.	superheating
T	refer to the Turbine of the IBC
TM	total module
w.f.	working fluid
w.h.	waste heat

Abbreviations

BC	Brayton cycle
BSFC	brake specific fuel consumption [g/(kWh)]
CS	combined scheme (IBC plus ORC)
CS Reg	CS with regenerative ORC
HE	heat exchanger
IBC	inverted Brayton cycle
KC	Kalina cycle
LCOE	levelized cost of energy [$/MWh]
MCT	module costing technique
n/a	not applicable
OFC	organic flash cycle
ORC	organic Rankine cycle
ORC Reg	regenerative ORC
R&D	research and development
sCO_2	supercritical CO_2 cycle
SRC	steam Rankine cycle
tCO_2	transcritical CO_2 cycle
TEG	thermoelectric generator
TIT	turbine inlet temperature
TOL	thermal oil loop
TRC	trilateral Rankine cycle

parameters tCO_2 is preferable than ORC; however, the second law efficiency is comparable, and the total product unit cost is slightly better for the combination of sCO_2 with ORC. Ref. [9] has studied eight different configurations of sCO_2 for various high-temperature WHR applications, with the total cycle efficiency varying from 20 to 27.5% approximately, and LCOE around 100 $/MW for the temperature corresponding to the nominal case of the present work. Yari (2015) [10] compared Kalina cycle with ORC and its transformed version, so-called trilateral Rankine cycle (TRC) characterized by triangle shape of T-S diagram due to the expansion initialized from the saturation line. The authors concluded that although ORC is losing TRC in maximum optimal obtained power (from 14 to 35 percent difference depending on the assumed expander efficiency) but TRC superiority in optimized system product cost depends on expander efficiency differently (from 3% lower values to 10% higher). KC has lost both in power and cost optimizations. Finally, the authors concluded that ORC is the best option for low-temperature heat utilization. Interestingly, these conclusions are less favorable for TRC than the results of the earlier works about TRC, e.g. of Fischer (2011) [11]. Later, Nemati (2017) [12] compared KC with ORC specifically for the WHR, reporting 22.5% superiority of the ORC over KC in generated power. IBC is a technology which has not found a strong field of application yet; however, it has a potential for high-temperature cases (Bianchi 2011 [13]). This technology will be discussed below in more details. At the same time, the application of conventional Brayton cycle for WHR is a rare case. However, it was just recently studied by Nader (2018) [14] who reported 5.5% to 7% fuel economy for the intercooled configuration in comparison with the base case. OFC technology is a relatively new field of study and discussed in few works. E.g., Lee (2016) [15] compared OFC in two configurations with ORC, concluding the advantage in produced net power of the OFC with two-phase expander over ORC for the evaporation temperature below 110 °C. Baccioli (2017) [16] defined a new architecture to reduce OFC equipment cost for the temperature of heat source in the range 80–170 °C. The Stirling cycle for WHR was not so comprehensively investigated (e.g., reviewed by Wang K. (2016) [17]). Both OFC and Stirling are reported as having a good prospect but facing specific engineering problems of certain components, that is why they do not have sufficient practical validation. Usage of the non-mechanical ways of energy harvesting for WHR purpose has also been studied (e.g., Zhang Y. (2015) [18]) (The results have shown that this solution is suitable only for specific cases due to the essential limitations of efficiency and heat transfer parameters (Jouhara (2018) [4]). However, Jouhara expects sufficient growth of the efficiency of TEGs in the nearest future. This small overview shows that a lot of various WHR technologies are under the intent attention of the scientific community. At the same time, ORC holds the leading position as one of the most efficient, reliable, and cost-effective solutions for temperatures below 400 °C.

On the other hand, the study of reviews and dedicated technical papers mentioned above has shown that in the range of exhaust temperature between 400 °C and 650 °C there is a gap in available, efficient WHR technologies as ORC has specific limitations on reaching higher efficiencies for the higher temperatures. Summarizing the large scope of researches in the field of WHR generating facilities based on ORC, Lecompte (2015) [5] has studied a group of works dedicated to the high-temperature ORC: in the range of about 250–400 °C; this is a low-middle temperature waste heat according to Zhai (2016) [19] classification. Two main factors govern the upper boundary of this

temperature range. One is the physical properties of available organic fluids suitable for this purpose with attention to the critical temperature, temperatures of stability, flammability, and condensation pressure. Another one, driven by operational requirements from the beginning, is the practical infeasibility of the schemes without an intermediate thermal oil loop (TOL) (Shi (2018) [20]). The maximum working temperature of found thermal oil is below 400 °C (e.g., Therminol VP-1 [21]). Thus, the connection between efficiency and maximum temperature of a thermodynamic cycle reveals the incomplete use of heat potential when ORC utilizes the exhaust with the temperature above 400 °C. Bianchi (2011) [13] derives the work with a similar conclusion.

However, studies show that many industrial processes and engines release energy flows to the atmosphere at a higher temperature. Heat treating furnaces for a range of materials, drying and baking ovens, cement kilns, and also gas turbines and reciprocating engines produce exhaust gases at temperatures from 400 °C to 650 °C. Table 1 represents the summary of the sources in the temperature range of interest for this study. For the United States, the total heat (referenced to 25 °C) containing in industrial waste flows at medium temperature (230–650 °C) exceed $132{\cdot}10^9$ kWh/year ([22]) that can be converted to more than $19.8{\cdot}10^9$ kWh/year of electrical energy assuming the average efficiency of conversion equal to 15%. This number, which exceeds 0.5% of total annual US electricity consumption [23], show sufficient prospects for the utilization technologies specially sharpened to this temperature range. As the temperature limitation for the ORC, discussed in the previous paragraph, equals to 400 °C, this work has a focus on the temperature range from 400 °C to 650 °C.

Among all sources of waste heat, the power-generating engines require separate attention. In opposite with technological facilities, their primary purpose is power production. It means that the appearance of additional power capacity does not brings changes neither to the business neither technical process. The same arguments are generally correct for the vehicle engines and other prime movers like gas turbines of gas compressor stations. In the authors' opinion, this is the main reason for the essential interest of the R&D and scientists to the topic of WHR in this area. Optimizations and techno-economic assessments of ORC for WHR after different kinds of engines are widespread in scientific literature and public industrial reports. Examples of detailed studies of such cases are reported in the study of Lion (2017) [6] and Sprouse (2013) [32], both reviewed and studied not only thermodynamics and economics but also the part-load under typical operation schedule for a heavy-load truck. In the review, Lion [6] reports ORC as the most applicable technology for this purpose with achievable fuel economy up to 10% at full load. Sprouse [32] has a similar conclusion of the review, also underlining that there is no ideal working medium optimal for all cases. In the work of Yue (2014) [33], the influence of the ORC integration to the performance of 2 MW Diesel engine was studied. The results showed that not only the efficiency of the ORC module but the corresponding efficiency drop of the topping cycle appearing due to backpressure growth should be considered. Xu (2019) [34] also has noted the importance of this factor.

IBC is a technology, which is more suitable for high-temperature WHR than ORC from the perspective of the usage of high-temperature gases. In the scientific literature, it is studied in different configurations for a variety of applications. The standalone operation of IBC as a power generating unit was studied in papers of Henke (2013) [35], Agelidou (2017) [36], and Valdés (2016) [37]. Henke [35] has analyzed the influence of temperatures in different points of the cycle and water condensation in the duct and concluded the unclear prospects of the technology due to low efficiency and high capital cost. However, this work was continued in the paper of Agelidou (2017) [36] with experimental data of small power-generating facility (about 1 kW). Valdes (2016) [37] compared IBC with BC and sCO2 for the micropower generation (about 1 MW) and estimate the IBC results as the worst because of its lower efficiency. Another group of researches is dedicated to the bottoming application of IBC with conventional BC in different configurations: Venkata (2012) [38], Matviienko (2016) [39], Chen (2017) [40], for instance. In Venkata (2012) [38], the focus lies mostly on the exploring the use of teaching-learning-based technique, also adopting artificial "bee colony" algorithms, for the optimization of combined BC-IBC system. Matviinko (2012) [39] has investigated the BC-IBC combination for the marine propulsion system, claiming the positive results of the system at part-load regimes due to the variable area nozzle. Chen (2017) [40] declared the maximum resulting average brake specific fuel consumption (BSFC) improvement equal to 3.02%, also discussing the optimal choice of pressure ratio for the conditions of standard driving cycle. Bianchi (2005) [29] studied this combination from the point of view of the base BC repowering, standing in the origin of the modern study of IBC. As a power-generating or repowering solution going after reciprocating engine, the IBC was studied mostly as an addition or an alternative to turbo-compounding. Copeland (2016) [40] and Hu (2016) [41] investigated the thermodynamic potential of different versions of this scheme. In his later work, Bianchi (2011) [13] in the review of bottoming cycles for electricity generation emphasized the potential of IBC for CHP application with the temperature of primary exhaust higher than 400 °C. Also, several non-conventional applications of the cycle were analyzed; Weber (2010) [42] studied a combined scheme of IBC and steam Brayton cycle applied with the chemical looping combustion reactor. All mentioned works report the presence of both the advantages and disadvantages of the IBC for WHR or power generation. One of the main questions to IBC is a high unused energy potential of the utilized exhaust gas.

Concluding this overview, it may be underlined that, on the one hand, there is a group of technologies producing high-temperature exhaust (400–650 °C) and suitable for WHR. Specifically, WHR from exhaust gases of the power and automotive internal combustion engines (ICE) worth attention. On the other hand, existing technologies in this

Table 1
Exhaust temperature for different technological processes.

Source	$T_{w.h.}$, °C	Reference	Comments
Reciprocating engines	340–620	GE™ [24], CAT™ [25]	
	550–660	Elfasakhany (2016) [26]	Acetone-gasoline mix.
	500–750	Masum (2014) [27]	Alcohol-gasoline mix.
	315–600	Zeb (2017) [28]	
Gas turbines	440–625	Bianchi (2005) [29]	Elec. power < 10 MW
	370–540	Zeb (2017) [28]	
Heat treating furnaces	425–650	Zeb (2017) [28]	
Drying and baking ovens	230–600	Zeb (2017) [28]	
Cement kilns	280–450	Shabana (2013) [30]	
	450–620	Zeb (2017) [28]	
Glass industry	500	Campana (2013) [7]	
Petroleum coke production	480–540	Neeharika (2012) [31]	
Catalytic crackers	425–650	Zeb (2017) [28]	

field show low efficiency and high cost because of some essential obstacles for being used for high temperatures. To cope with this challenge, a solution based on the combination of ORC and IBC is being suggested; it brings the growth of WHR system efficiency and attractiveness of the investment into WHR projects.

Previously, the author worked with IBC, which has a separate introduction in the paper as IBC is not so commonly known. The idea to improve IBC with ORC integration is not completely new (e.g., IP disclosure in [43]), but was not studied in the scientific literature. This work demonstrates a comparative analysis of this scheme benchmarking it versus the conventional ORC. The realization of the model was performed in Aspen Hysys 9 software with usage of its standard 1-D components. As a target case, the Internal Combustion Engine of suitable capacity was chosen. Additionally, an authentic approach to the estimation of the IBC turbomachines' efficiency was introduced. The negative influence of the ORC to the primary engine emphasized in Yue (2014) [33] is not taken into account to keep the work simpler. However, the introduction of IBC compensates this influence and gives one more advantage for the proposed scheme, so it is a conservative assumption of the comparison.

In this work, the investigated combined IBC-ORC scheme, which, to the authors' best knowledge, was never systematically studied before, is compared with the ORC-based solution with orientation on the case-study of a stationary gas-fired reciprocating engine. To define the best result on the in-house simulator, the ORC model was designed and optimized for three different fluids, considering cycle limitations from Quoilin 2012 [44]. This approach provides preliminary techno-economic feasibility assessment of the ORC and differs from pure thermodynamic estimations. The fluids correspond to three levels of critical temperature. The ORC was built in two configurations: regenerative and non-regenerative ORC and optimized for the properties of inlet exhaust gas corresponding to the nominal case (temperature 520 °C). The next step was the comparison of the efficiency-optimized combined scheme in two configurations: with regenerative ORC and without regeneration, and two configurations of the conventional ORC. The efficiency of the IBC turbomachinery was assessed by a simplified technique based on Reynolds number adapted for this specific case (see Section 2.2.5 and Appendix C). The inlet temperature of the exhaust gas was varied from 470 to 570 °C. The working medium for all cases is pentane, as it was defined in the previous step as the best option. The sensitivity analysis for the most important parameters was performed to estimate the influence of assumptions of the components' parameters on the results. Additionally, the optimal characteristics of IBC for different temperatures are shown, as well as the condensation rate in the subatmospheric duct and its influence on the IBC performance under different turbine pressure ratios. The third part of the results is dedicated to the LCOE evaluation for four potential investment projects based on the investigated schemes. LCOE is shown for the different capacity factor[1] (CF) values of the potential facility at the nominal inlet parameters. These results are obtained after LCOE-based optimization.

Summarizing, the contribution of this work is to provide the first systematic study of the combined IBC-ORC scheme. It includes a comparative analysis versus the most deployed WHR technology – the ORC, a sensitivity analysis from external parameters (inlet temperature) and model assumptions, and an LCOE calculation for different CF of the facility. The methodology used in this first assessment is based on mass and energy balance to define an optimal design of the scheme, by considering actual limitations for ORC (adopted from the literature), flue gas dewpoint, and a method for the estimation of IBC turbomachinery efficiency. Applied reliable commercial software enables not to be focused on the components' models but to get a credible assessment of the whole new system. This work gives the first estimation both thermodynamic and economic of the operation of such a scheme, and its potential for further research. It suggests an optimized configuration for the advanced WHR system by providing useful information for the design of numerical or physical models of this high-efficiency and cost-effective high-temperature WHR scheme.

[1] Capacity factor – a unitless ratio of the generated power output to the maximum possible output (8760 h of operation for one year period)

2. Model description

In this paragraph, the model of the WHR system is reported, with a focus on the description of the IBC.

2.1. Inverted Brayton cycle

Inverted Brayton Cycle is another version of the conventional Brayton cycle but with a turbine immediately in the inlet for the hot medium. The medium may heat up in the combustion chamber, in the heat exchanger (HE) from a source of waste heat; or the system may directly receive exhaust gases from an engine or some technological process. Fig. 1a and b show T-S diagram and generalized scheme of the cycle. The hot gas performs useful work in the turbine (process 2–3), where it is cooled down correspondingly with the pressure decrease and goes to the cooler under subatmospheric pressure (point 3). Being cooled down to the temperature close to ambient (point 4), the gas flow from the cooler recovers pressure back to the atmospheric level in the compressor (process 4–5) subsequently having the temperature growth during this process; after that, the gas is released to the atmosphere (point 6 at the T-S diagram).

Subatmospheric pressure provides both advantages and disadvantages to the scheme, which were summarized in the previous work Abrosimov (2017) [45]. Additionally, for the WHR application with the direct intake of exhaust gases, it can be underlined that no external work is needed for pushing heat-containing medium through the system due to the compressor, which drives this flow. In other words, the system does not create back-pressure for the primary engine or another gas source.

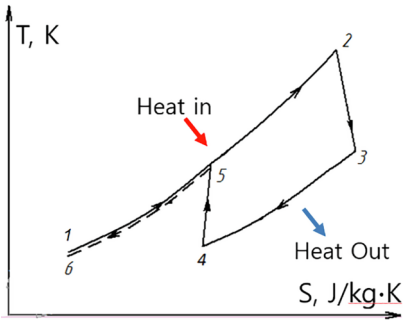

Fig. 1a. T-S diagram of IBC. (1–2) – heat addition; (2–3) – turbine expansion; (3–4) – cooling; (4–5) – compression; (5–6) – release to atmosphere.

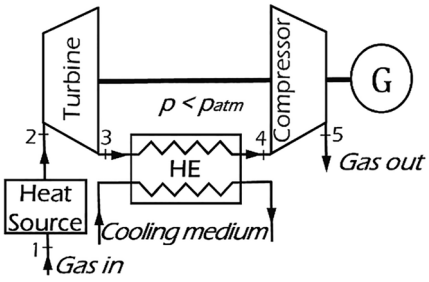

Fig. 1b. Basic scheme of IBC for WHR.

2.2. Case study technical description

This chapter presents the technical aspects of the work. In the beginning, the targeted case-study is described. Further, the investigated scheme receives a detailed introduction, as well as the ORC, which was studied to provide the benchmark for the comparison. Then, the simulation assumptions and adopted limitations are listed. Finally, a specific methodology for estimation of efficiency of bladed machines in conditions of IBC is presented.

2.2.1. Targeted application

The present work orients to the heat utilization from the reciprocating engine exhaust. Study of Diesel and gas-fired power and driving engines enables to define a range of exhaust temperature on nominal load (GE™ [24] and CAT™ [25]). Reciprocating internal combustion engines up to 1400 kW capacity (e.g., Waukesha VHP L7044GSI S5) have exhaust temperatures that can reach up to 620 °C. This observation motivates authors to assess the proposed technology for the primary engine from the capacity range of 500–1400 kW and exhaust temperatures from 400 °C to 600 °C. And the focus is on gas-fired engines, which have been becoming more and more important in power production and propulsion systems. Summarizing, the supposed nominal case of the source of the waste heat in this study is a gas-fired reciprocating engine with the power of about 1 MW with the nominal exhaust temperature 520 °C and gas flow rate 1.47 kg/s. Its chemical composition presented in Appendix A corresponds to the natural gas burning at air combustion coefficient α = 1.2 [46], and air humidity equals 60%.

The useful power is employed by an electric generator. On this first stage, useful application of heat was not considered, leaving the CHP solution investigation for the next steps.

2.2.2. Investigated combined schemes

The layout and T-S diagram of the combined IBC-ORC scheme with non-regenerative ORC (CS) is shown in Fig. 2a and b. Fig. 3 presents the combined scheme with regenerative ORC (CS Reg); the difference in the operation of these two configurations is described below. In the following paragraph, the processes that occur in the first configuration are illuminated.

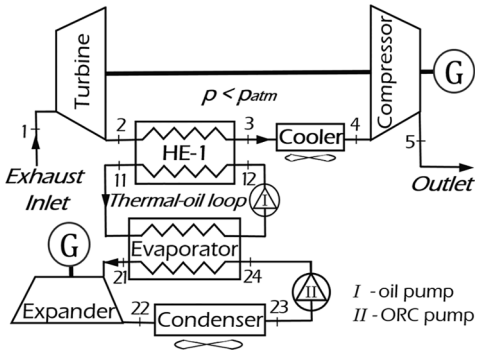

Fig. 2a. Scheme of the combined cycle.

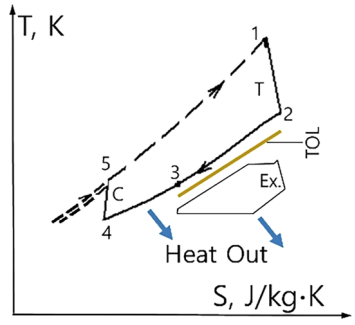

Fig. 2b. T-S diagram of the combined cycle.

In point 1 of Fig. 2, hot exhaust gas, assumed to be at atmospheric pressure, enters the duct of the WHR system expanding in a gas turbine to the point 2 of the sub-atmospheric pressure and lower temperature. The usual values for the case studied are the pressure from 45 to 55 kPa what corresponds to the turbine inverse pressure ratio $\pi_T = 1.8–2.4$ easily achievable by one stage radial machines, where $\pi_T = p_{T.in}/p_{T.out}$. After the Turbine, the gas goes through the gas-to-thermal-oil heat exchanger (HE-1), which is the pass of the heat to the ORC part of the cycle, and finally, it is cooled down in the air Cooler to 35 °C – point 4. Condensation takes place in the Cooler, so a separator was introduced to the scheme after the Cooler. The separator is not presented on the scheme. The cooled gas is compressed up to the atmospheric pressure in the compressor and directed to the outlet. The compressor pressure ratio (π_C) is slightly higher than the turbine one, where $\pi_C = p_{C.out}/p_{C.in}$. Thermal oil from the HE-1 (point 11) goes to the Evaporator arriving to the oil pump (II) at point 12.

Working fluid heated up in the Evaporator with the super-heating not less than 5 °C for the sake of the process stability (point 21) goes to the Expander, which in the studied case is assumed to be a radial turbine, where the pressure and temperature decrease. Then, the low-pressure vapor in point 22 is cooled down in the air-cooled Condenser. Cooling air temperature is supposed to be 20 °C. Hence, the lowest possible temperature of working fluid considering the pinch limit 5 °C may go a little below 30 °C. The observed range of the pressure after the Condenser is above 70 kPa, which fulfills the lowest technically feasible limit of 20 kPa set by (Quoilin (2012) [44]). After the Compressor, a pump (I) increases the pressure of the medium to the 2500–3000 kPa and directs the working fluid to the Evaporator.

The combined scheme (Fig. 3) equipped with regenerative ORC (CS Reg) differs from the basic one in the values of temperatures in some of the key points of ORC. Temperature before the Condenser is higher as well as before the Evaporator due to heat exchange of flows in the regenerator (Regen. – in Fig. 3). It leads to an increase of the lowest temperature of the oil loop and, thus, gas temperature after HE-1. The cooling power of the Cooler must be increased to ensure that the temperature of the gas entering the compressor is equal to referenced 35 °C.

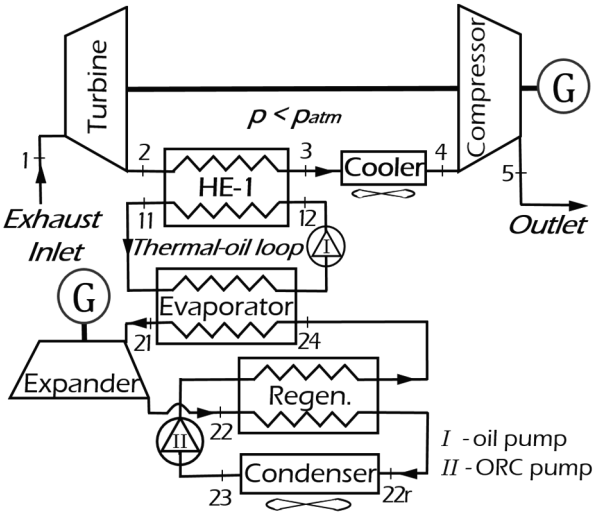

Fig. 3. Scheme of the combined cycle with regenerative ORC part.

2.2.3. Organic Rankine cycle

The above mentioned combined scheme was studied and benchmarked against an ORC-based solution, which is currently the

technology with higher deployment. The non-regenerative cycle was also considered to make the comparison inclusive. The scheme of the non-regenerative ORC is presented in Fig. 4. In this system, the heat from the exhaust gas flow is transmitted in the HE-1 to the working medium of the cycle through the TOL with similar parametric assumptions.

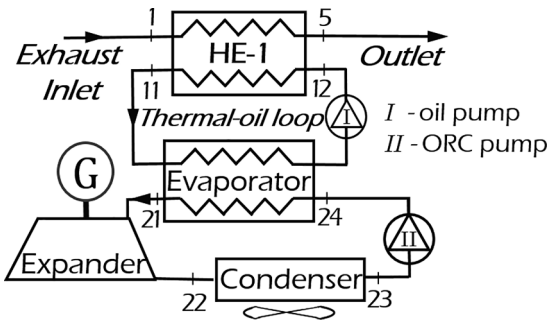

Fig. 4. Scheme of ORC.

2.2.4. Assumptions and limitations

Assumptions for equipment type, losses, efficiencies, some fixed temperatures, and heat transfer parameters are presented in Table 2 and commented below.

Equipment type. The type of heat exchangers was chosen from the list available in Turton (2008) [47] based on the fluids, pressure, heat flow, and practices established in this technical area. Turton's book was used for economic assessment (see chapter 2.4). Radial compressor and turbine for IBC part are suitable for the investigated range of flow rate, pressure ratio, and temperature (Dixon (2010) [48]). ORC expander type was chosen based on data in Quoilin (2012) [44].

Losses. Here, the relative drops of pressure in the HEs caused by mechanical losses are listed. Relative pressure drop is defined as: $\overline{\Delta p} = \Delta p/p_{in}$.

Isentropic efficiencies of bladed machines. Efficiencies of the bladed machines in the IBC part are discussed in chapter 2.2.5. ORC expander efficiency corresponds to values in literature.

Heat transfer coefficient. The parameter was defined, relying on the data in Sinnott (2005) [49]. The Evaporator was simulated as a group of three different HEs representing pre-heating, evaporation, and superheating processes in the evaporator. An own separate value of $U_{overall}$ corresponds for each of these HE. The resulting value for the whole Evaporator lies in the range indicated in Table 2 and depends on other design parameters of the system.

Cooling air temperature and the *temperature of cooled gas before the Compressor* correspond to an assumed temperature of the coolant in the Condenser and the Cooler, and an assumed temperature before the compressor, respectively. The second value is fixed to reduce the number of variables in the simulation, and it is higher than the lowest temperature of the working fluid in the condenser because of worse heat-exchange conditions: the phase transition occurs in the Condenser, but, in the Cooler, an only small fraction of water has phase change.

Additional specificities are listed below:

- The negative impact of ORC on the primary ICE caused by the back-pressure was not considered. The back-pressure appears due to the resistance of the heat exchanger located in the exhaust gas duct (Yue (2014) [33]). For the investigated CS, in the opposite, a conservative assumption was made to consider this resistance been compensated by the Compressor. The validity of the assumption conforms to the practical absence of the affecting on the primary engine due to the Compressor, which provides atmospheric pressure in the cross-section engine-CS.
- Heat losses to the atmosphere are neglected for all components of the schemes.
- Power consumption of the heat removal process in Condenser and gas Cooler ($P_{cooling}$) is subtracted from the power of the turbine based on the assumption of 17 W per kW of removed thermal power corresponding to the air heat sink (Antonelli (2016) [50]).
- Subcooling in the Condenser is 1 °C to guarantee the absence of vapor in the Pump.
- Maximum evaporation temperature is at least 15 °C below the critical temperature of the working medium to guarantee stable operation.
- Minimal superheating temperature is equal to 5 °C with the same purpose.
- To consider the presence of the generator, the on-the-shaft power of the turbine-compressor unit of IBC and expander of ORC were multiplied on the efficiency of the generator equal to 96%. Mechanical losses are also included in this coefficient.
- In Aspen HYSYS, Peng-Robinson equation of state for flue gas, RefProp equation of state for organic fluids, UNIQUAC – for thermal oil, are chosen (Baccioli (2018) [51]).
- Aspen HYSYS components are standard and have basic thermodynamic models; the basic equations for turbomachinery and heat exchangers are given in Appendix B.

Table 2
Assumed values for the parameters of the three schemes.

Line	ORC, ORC Reg	CS, CS Reg
Equipment type		
- HE-1	Cross-flow shell and finned tube	Cross-flow shell and fined tube with cylindrical housing
- Evaporator	Bayonet shell and tube	
- Condenser	Air cooled finned tubes	
- Regenerator	"Multiple pipe" shell and tube	
- Cooler	n/a*	Air cooled finned tubes
- Turbine, compressor, expander	Radial bladed machines	
Losses (relative pressure losses)		
- HE-1	0	0.035
- Evaporator, fluid side (non-Reg|Reg)	0.03|0.025	
- Evaporator, oil side	0.005	
- Condenser	0.035	
- Regenerator, HP side	0.02	
- Regenerator, LP side	0.03	
- Cooler	n/a	0.02
- Separator	n/a	0.01
Isentropic efficiencies of bladed machines		
- Turbine	n/a	86%
- Compressor	n/a	83.8%
- Expander	80%	
Efficiency of generator	96%	
Heat transfer coefficient ($U_{overall}$), W/(m^{2}K)		
- HE-1	130	
- Evaporator (heating-evaporation-superheating)	400–500 (550-680-100)	
- Condenser	550	
- Regenerator	150	
Cooling air temp/ambient temperature, °C	20	
Temperature of cooled gas before the Compressor, °C	n/a	35

* n/a – not applicable.

2.2.5. Efficiency of bladed machines in sub-atmospheric conditions

The efficiency of Turbine and Compressor were assigned based on the specific simplified approach. First, the efficiency of the machines for the case of BC application was chosen from engineering practice. Then, BC and IBC machines of the equal gas flow rate were compared, and the

values of efficiency were corrected for the IBC application. Henke (2013) [35] has considered the following correlation based on Reynolds number as the most suitable for the case (Eq. (1)).

$$\frac{1-\eta_1}{1-\eta_2} = \left(\frac{Re_2}{Re_1}\right)^n \mathrm{n} = 0.06 - 0.2 \tag{1}$$

where n depends on Raynolds number.

However, while Henke applies the formula with n = 0.06, in this work, a higher value (n = 0.2) for the efficiency was assigned to avoid being too optimistic in the conditions of methodological uncertainty. Finally, the formula applied in this work, considering the correlation between π_T and Reynolds number (Eq. (1)), is the following:

$$\eta_{IBC} = 1 - {\pi'_T}^{0.1} \times (1 - \eta_{BC}) \tag{2}$$

Appendix C contains the full derivation of this equation. Table 3 provides data about efficiency values for BC and IBC taken as an initial assumption and calculated based on it correspondingly.

Table 3
Assumed efficiency of turbomachines in BC and IBC conditions.

	BC	IBC	Parameter
Turbine	87% (2.1)	86% (2.1)	$\eta_T(\pi'_T)$
Compressor	85% (2.25)	83.7% (2.25)	$\eta_C(\pi_C)$

2.3. System and cycle efficiency introduction

This study orients on the final results of the system performance in the exploiting of available heat, so the main parameter used is net system efficiency:

$$\eta_{sys} = \frac{P_{net}}{Q_{av}} = \frac{P_{gross} \times \eta_{gen} - P_{cooling} - P_{pump}}{(H_{in} - H_{amb}) \times \dot{m}_g} \tag{3}$$

P_{gross} corresponds to the sum of shaft powers of the turbine-compressor unit and the ORC expander. The cycle efficiency, which is used for the analysis of ORC performance is standard:

$$\eta_{ORC.cycle} = \frac{P_{ORC.net}}{(H_{wf.in} - H_{wf.out}) \times \dot{m}_{wf}} = \frac{P_{Exp} \times \eta_{gen} - P_{ORC.cooling} - P_{ORC.pump}}{(H_{wf.in} - H_{wf.out}) \times \dot{m}_f} \tag{4}$$

The sum of power consumed for cooling ($P_{cooling}$) and pumping of ORC working fluid and oil in TOL (P_{pump}) is named as the ancillary consumption or Utilities.

2.4. Economics assessment methodology

An economic evaluation of the proposed scheme and its comparison with ORC based facility were provided with the use of LCOE approach. It estimates the electricity market price, which makes the project profitable with minimum acceptable parameters of investment return on the period of project life. The formula for calculation of this factor is following (Pili (2017) [52]):

$$LCOE = \frac{C_{tot} + \sum_{i=1}^{t} \frac{C_{O\&M.i}}{(1+r)^i}}{\sum_{i=1}^{t} \frac{\Delta E_i}{(1+r)^i}} \tag{5}$$

where C_{tot} is total capital investment cost, $C_{O\&M}$ is operation and maintenance cost (3% of C_{tot}), t is run-time of the plant in years (20 years), r stands for the discount rate (7%), ΔE is net energy generated by the system over one year. For simplicity, single-tranche capital investments from own funds are considered. Taxation, year-by-year growth of $C_{O\&M}$, decrease of capacity, as well as insurance payments, are not included in the model. As so, ΔE and $C_{O\&M}$ from the Eq. (5) are constant. The interest rate is assumed based on typical values for this field of interest Gant Thornton LLP (2018) [53].

The capital cost of components was calculated following the module costing technique (MCT) briefly but exhaustively described in Toffolo (2014) [54], for instance. Mostly, the cost-functions are taken from Turton (2008) [47] besides the condenser, generators, and separator, which are not presented in this book. Sufficient formulas for the Condenser and the Generator were taken from Smith (2005) [55] and Toffolo (2014) [54] respectively following Lemmens (2016) [56] in these approximations. The separator was assessed with an assumption from Garrett (2012) [57]. Cost-functions for all components, as well as the coefficients of these functions, are summarized in Appendix D. To bring all values to current prices in the same currency ($ 2017 year), the official open historical data for CEPCI ($CEPCI_{2017}$ = 567.5) [58] and $/€ exchange rate [59] were used. The final total cost is derived from the sum of the components cost with multiplication over 1.18 corresponding to the system mounting costs, including the cost of TOL (Turton (2008) [47]).

2.5. Optimization details

The optimization applied to the studied combined scheme and ORC enabled finding the best combinations of variable parameters for them. In the first part, the objective function was the system efficiency, and in the second, economic part, it was LCOE. The constraints for the optimization were similar for both cases, but for the second one, resulting value of parameters usually laid aside from the limiting values as they give high costs of components. Table 4 presents the constraints applied in the optimizations. Minimal pinches were dictated by the technical feasibility of such HEs, minimum temperature till T_{cr} limits the evaporation temperature in ORC and determine the operational stability of the system (Delgado-Torres (2007) [60]). The limit for the superheating is chosen by relying on the commonly known technical practice.

For the optimization, a standard Aspen Hysys optimizer was used with the BOX scheme and 2e-5 tolerance. “Maximum change per iteration” parameter was varied in the range 0.5–3 to obtain global extrema with higher precision.

Table 4
Constraints for the objective functions of the optimization.

Constraint	Value
Minimum pinch HE-1, °C	30
Minimum pinch Evap, °C	15
Minimum pinch Condenser, °C	5
Minimum pinch Regen, °C	15
Minimum temperature till T_{cr}, °C	15
Maximum oil temperature, °C	380
Maximum superheating, °C	40

3. Results, sensitivity, and discussions

This section presents the results. Firstly, the best working fluid for ORC is identified based on the achieved system efficiency. Then, the results of the system efficiency optimization are presented together with LCOE optimization. The sensitivity analysis of the results is also demonstrated.

3.1. Choice of the working fluid for the organic Rankine cycle

The comparison of the suggested combined scheme with ORC was started by defining the optimal features of the ORC-based system simulated on a domestic model. Two configurations have been studied: regenerative and non-regenerative ORC. For the targeted application, the power of the ORC lies in the range suitable for the radial inflow turbines as an expander (Quoilin (2012) [44]). In his work, Quoilin has

also formulated the parametric limits for different types of ORC expanders, including radial turbines, for several working fluids. Three fluids with different level of critical temperatures (T_{cr}) were chosen, distinguished as low T_{cr} fluid – R245fa, medium T_{cr} fluid – pentane, and high T_{cr} fluid – toluene. Built model of the ORC considers Quoilin's limits to define the possible ranges of evaporation and condensation temperatures. Fig. 5 shows obtained results for these three fluids with the employment of regenerative (ORC Reg) and non-regenerative (ORC) cycles.

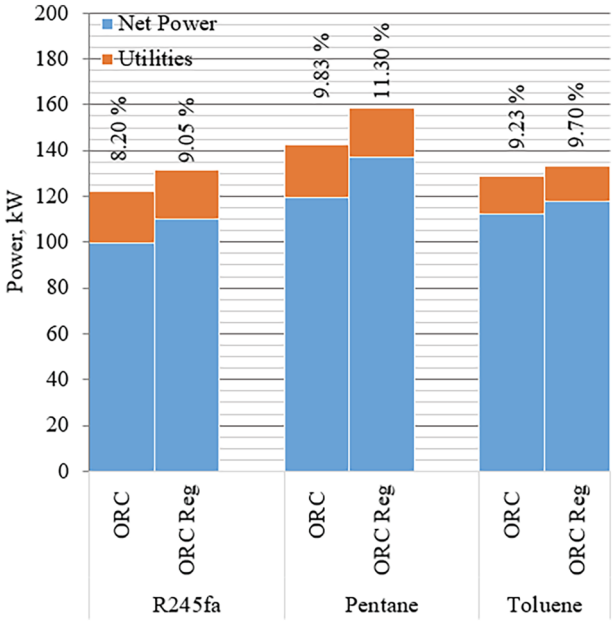

Fig. 5. Power and system efficiency of ORC and ORC Reg with different working fluids employed.

Table 5 shows the resulting parameters of the η_{sys}-optimized systems with three studied fluids. The maximum generated power is demonstrated by regenerative ORC with pentane as the working fluid, although its critical temperature is far below the maximum available temperature of the cycle (380 °C). Interestingly, the use of toluene yields a lower performance level, even though it has a much higher critical temperature which defines higher evaporation temperature and also permits a lower relative auxiliary consumption because of the higher energy density it carries (see Share of utilities in Table 5). The explanation of this fact is following: according to the Quoillin limitations the lowest condensation temperature acceptable for toluene (63 °C) is higher than the lowest available temperature of the system (around 25 °C); this implies that a lower amount of energy is received from the exhaust gas flow in comparison with the lower-temperature pentane case. The cycle efficiency for toluene could be potentially higher, but the smaller amount of energy transmitted to the cycle makes the system efficiency of the toluene cycle lower than the pentane one. In Table 5, this difference in cycle efficiency is not observed because the optimization has the overall system efficiency as the objective function but not cycle efficiency. In the work of Lecompte (2015) [5], the efficiency of the external irreversible Carnot cycle is introduced instead of the standard Carnot efficiency to make the preliminary estimation of such WHR systems. For the same reason of the small amount of energy transmitted, the optimal condensation and evaporation temperatures for toluene are at the lower boundary of the prescribed range corresponding to the lower evaporation pressure. Meanwhile, this boundary is determined by an acceptable condensation pressure (20 kPa) [44]. Therefore, regenerative ORC with pentane as the working fluid is the best competitor for the studied system due to its higher system efficiency and larger net output power.

Table 5
Parameters of ORC of two configurations with different working fluids.

Line	R245fa		Pentane		Toluene	
	ORC	ORC Reg	ORC	ORC Reg	ORC	ORC Reg
Net power, kW	99.7	109.8	119.8	137.3	112.2	118.0
η_{sys}, %	8.20	9.05	9.84	11.30	9.23	9.70
η_{cycle}, %	13.0	16.47	15.5	21.2	15.7	19.4
Share of utilities, %	18.4	16.2	16.3	13.38	13.0	11.3
p_{evap}, bar	28.1	27.73	26.85	26.88	8.92	8.9
p_{cond}, bar	1.67	1.71	0.77	0.78	0.22	0.22
T_{evap}, °C	138.9	139	181.9	181.9	210.1	210.1
T_{cond}, °C	29.1	29.8	28.3	28.8	64	64
$T_{s.h.}$, °C	25.6	40	6.1	40.0	5	29.2
T_{out} (T_5), °C	74.6	134.2	74.5	153.8	108.7	172.3

3.2. Results of the efficiency optimization

Fig. 6 presents the performance of compared schemes operating in conditions of the exhaust in the temperature range around the nominal temperature (520 °C). These results are obtained after η_{sys} optimization following the parameters and constrains mentioned in previous chapters. The left axis corresponds to the column-chat of system power, the right upper one – to the lines of efficiency in the top half of the figure, the right bottom one – to the relative difference in power for each temperature related versus non-regenerative ORC. On the column-chat of the power, the useful power is presented by the blue column (for ORC) or the sum of the OBC (blue) and IRC (orange) column (for CS). The utilities are subtracted from the generated (gross) power of ORC and IBC in correspondence with the source of auxiliary consumption (ORC or IBC). For the nominal case, maximum observed values correspond to CS Reg with the P_{net} = 151.7 kW and η_{sys} = 12.49%, whereas ORC Reg has P_{net} = 137.0 kW and η_{sys} = 11.3%. Relatively, CS Reg overcomes ORC Reg on 10.6% and ORC without regeneration on 28.2%.

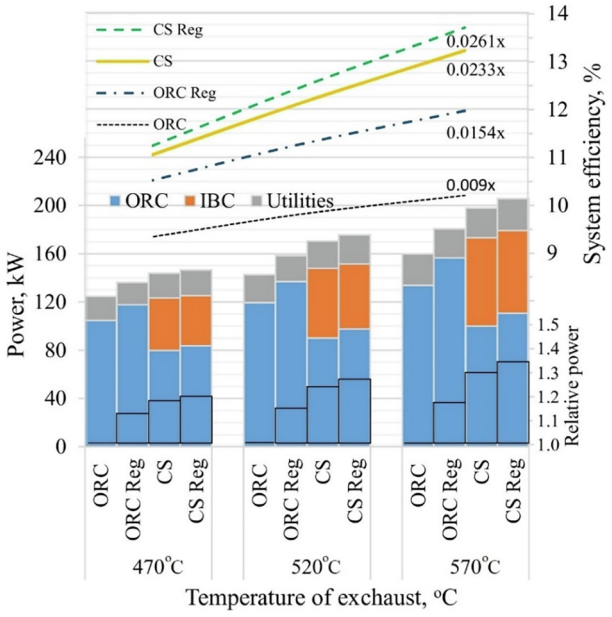

Fig. 6. System efficiency optimization results for ORC, ORC Reg, CS, and CS Reg for three different temperatures: 470 °C, 520 °C, and 570 °C.

One may see that for all three temperatures the growth of efficiency and power goes in the sequence: ORC, ORC Reg, CS, CS Reg. Additionally, with growing temperature, both absolute and relative

advantage of the CS schemes are increasing. It can be observed at the column-chart for power and the black stepped line in the bottom of chat for relative power as well as at the comparison of slope coefficients of the linear approximation. It means that higher temperature is preferable for combined scheme mostly as a result of the growing efficiency of IBC part. Performance data for the nominal temperature is presented in Table 6.

Table 6
Calculated parameters of the four schemes (nominal conditions).

Parameter	ORC	ORC Reg	CS	CS Reg
P_{gross}, kW	142.70	158.50	170.30	175.80
P_{net}, kW	119.50	137.0	147.8	151.7
η_{sys}, %	9.84	11.30	12.16	12.49
$\eta_{cycle.ORC}$, %	15.54	21.52	15.58	19.36
Π'_T	n/a	n/a	2.13	1.94
P_T, kW	n/a	n/a	210.4	186.9
π_C	n/a	n/a	2.23	2.07
P_C, kW	n/a	n/a	143.8	124.4
$r_{v.Exp}$	43.93	34.8	43.35	39.7
P_{Exp}, kW	142.7	158.5	103.7	113.3
$P_{Pump.ORC}$, kW	6.69	6.52	4.75	5.27
$p_{Con.out}$, kPa	77.1	78.5	76.1	78.5
$p_{Pump.out}$, kPa	2685.0	2688.0	2685.0	2688.0
$\dot{m}_{w.f.}$, kg/s	1.26	1.24	0.90	1.00
$\dot{m}_{oil}$, kg/s	1.36	1.11	1.02	0.95
T_{cond}, °C	28.3	28.8	27.9	28.8
T_{evap}, °C	181.8	181.8	181.8	181.8
$T_{Exp.out}$, °C	124	145.3	99.7	107.8
$T_{Con.in}$, °C	124	44.3	99.7	44.9
$T_{s.h.}$, °C	23	40	9	9.3
$T_{exh.g.out}$, °C	73.6	153.8	128.2	116.9
Δ_{Ev}, °C	15	15	15	15
UA_{Ev}, kJ/(K × s)	10.8	10.9	12.5	9.41
Δ_{Con}, °C	5	5	5	5
UA_{Con}, kJ/(K × s)	77.5	70.56	56.7	56.9
Δ_{Regen}, °C	n/a	15	n/a	15
UA_{Regen}, kJ/(K × s)	n/a	9.9	n/a	5.7
$\Delta_{HE\text{-}1}$, °C	30	30	30	30
UA_{HE-1}, kJ/(K × s)	12.7	9.6	13.2	12.5
Δ_{Cooler}, °C	n/a	n/a	15	15
UA_{Cooler}, kJ/(K × s)	n/a	n/a	9.3	11.7

3.2.1. Inverted Brayton cycle performance

One interesting aspect of IBC behavior should be articulated separately. The influence of condensation of water before the compressor have two opposite effects on the cycle performance. Due to the separator introduced before the compressor, the flow rate decreases for the compressor and its work goes down. But on the other hand, enthalpy of the gas decreases with the fall of the concentration of water vapor in the gas flow. These contrary impacts presented in more details in the next paragraph define non-trivial resulting dependence of IBC operation from pressure ratio (see Fig. 7). Also, the size and the pressure drop of the cooler are depending on the condensation rate, but this effect was not considered in the present study.

In Fig. 7, the effect of condensation on the gross power of IBC can be observed. Typical view of such power curve for IBC (and BC, in fact) is the convex curve with one absolute maximum. The high concentration of water in exhaust gases, as well as the presence of critical value of pressure (where the condensation ceases to occur according to the physical properties of the particular mixture of exhaust gases) in the considered range of pressure ratio, are causing an appearance of two local maximums at the graph. For different TIT temperature, the ratio between maximums changes. For TIT = 570 °C, the maximum in the no-condensation area prevails over the second maximum, in opposite with the cases with the lower TIT temperatures. This fact does not affect the optimal values of the pressure ratio in the optimizations of the studied combined schemes. That is because of the domination of the

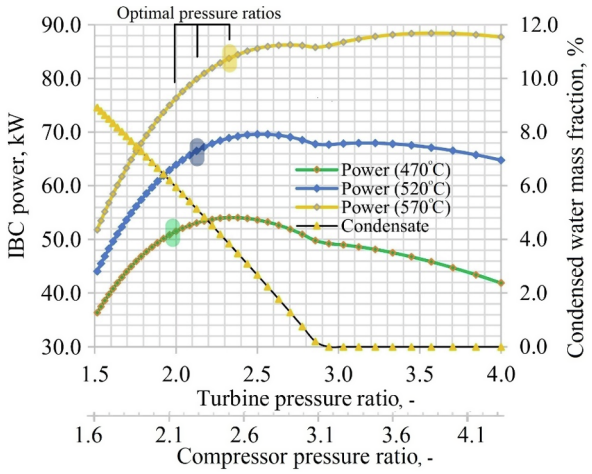

Fig. 7. IBC performance. Influence of water condensation.

ORC over IBC in power generation. However, for the studies of IBC without any bottoming cycle, this result is essential.

Relating to the right axis of Fig. 7, the line of the condensed water mass fraction for 35 °C temperature before the compressor shows that the critical value of pressure ratio is equal to about 2.9. It corresponds to the bend-point of the power curves. As the temperature before the compressor does not vary in this study, only one line of condensed water mass fraction is presented. Kennedy (2017) [61] discussed this issue showing the results conform to ours. In this study, the pressure ratio of a turbine (π'_T) is an originally variable parameter, but not the compressor pressure ratio (π_C) as in some other works. As so, the second horizontal axis was added to Fig. 7 to ease the comparison with the works of other researchers.

3.3. Sensitivity assessment for the nominal case

This section has the aim of studying the impact of assumed parameters on the simulation results because, on the one hand, the assumptions in this work have been made based mostly on the general engineering knowledge and values adopted in scientific papers so are not very precise. On the other hand, the sensitivity is another aspect of comparison of combined scheme versus ORC. Fig. 8 presents the influence of the change of different system parameters on system efficiency. The range of the analysis for each parameter is determined by the reasonable possibility of such a range, so the ranges are different. First, Fig. 8 shows the effects of the change of the single component parameter:

- CS Reg
  - Compressor efficiency
  - Evaporator pinch
  - ORC Expander efficiency.
- ORC Reg:
  - Pump efficiency
  - Evaporator pinch
  - ORC Expander efficiency.

In addition, it shows the resulting changes in the system efficiency caused by the simultaneous change of two parameters:

- CS Reg:
  - Evaporator pinch and HE-1 pinch
  - Efficiency of IBC turbine and efficiency of ORC expander
- ORC Reg:
  - Evaporator pinch and HE-1 pinch

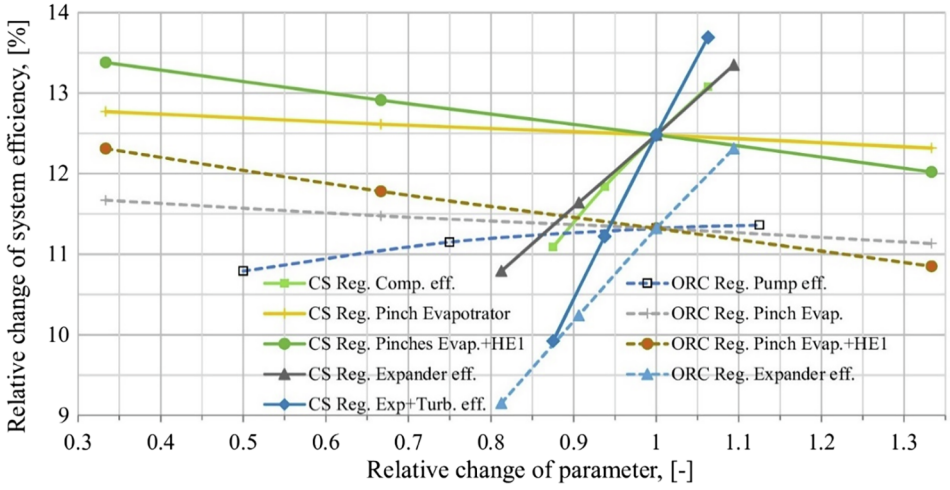

Fig. 8. Effect of change in assumed parameters of the scheme on the system efficiency for ORC Reg and CS Reg.

The dependence of the system efficiency from components parameters is mostly linear, as it can be observed in Fig. 8, besides the pump whose influence on the system efficiency drop accelerates with the decreasing pump efficiency. Efficiencies of the working machines are more influential than pinches of heat exchangers; however, it should be noticed that this comparison is not representative because of the different nature of these parameters.

The effect of the simultaneous change of turbomachinery efficiencies is substantial, especially for the combined scheme. For instance, a simultaneous 12.5% reduction of turbine and expander efficiency (the expander efficiency decreases from nominal 80% down to 70%) leads to the about 20% drop in system efficiency. The addition of the effect from a similar decrease in compressor efficiency gives a drop of about 33%. The last statement can be implicitly observed in Fig. 8. One may add the drop from the compressor to the reduction from the simultaneous decrease of turbine and expander efficiencies, what is possible due to their additivity under the assumption of their linearity, which one may apply for this approximate estimation. ORC Reg does not have a parameter, which can influence it in such a way. Extreme values of the graph in Fig. 8 are presented in Table 7.

Sensitivity analysis of system behavior shows that with a certain distribution of parameters of the components (mainly to say about efficiencies of bladed machines) the advantage of CS Reg may be leveled with ORC Reg or even turned opposite regarding system efficiency and LCOE.

Table 7
Sensitivity study data.

Parameter	Nominal value	Range of parameter	ORC Reg Range of η_{sys} ($\eta_{sys.nom}$ = 11.3%)	CS Reg Range of η_{sys} ($\eta_{sys.nom}$ = 12.49%)
η_{Comp}, %	83.6	73.3–89.0	n/a*	9.09–13.24
η_{Pump}, %	80	40.0–90.0	10.79–11.36	–
Δ_{Evap}, °C	15	5–20	11.67–11.13	12.77–12.32
+ Δ_{HE-1}, °C	15	5–20	12.31–10.85	13.38–12.02
Δ_{Evap}, °C	30	10–40		
η_{Exp}, %	80	65.0–87.5	9.15–12.31	10.79–13.35
+ η_{Exp}, %	80	70.0–85.0	n/a	9.92–13.69
η_{Turb}, %	86	75.2–91.4		

*n/a – not applicable.

3.4. Results of the economic optimization

To show the high-level comparative economic analysis, the LCOE-based optimization for potential investment projects based on the investigated systems was performed for nominal inlet parameters. The methodology of this approach and the assumptions of the model are presented in chapter 3.3. Here, in Fig. 9, the obtained values of LCOE are presented as a function of CF of the facility. Table 8 shows the parameters of the optimized system for CF = 90%. For other capacity factors, the optimization gave approximately the same values of varied parameters; so they are not presented in the table. The combined schemes show an advantage over the ORC schemes in LCOE and the efficiency simultaneously, what to be explained with a high share of the cost of heat exchangers in the capital cost of the systems. The distribution of expenses between system components is presented in Fig. 10.

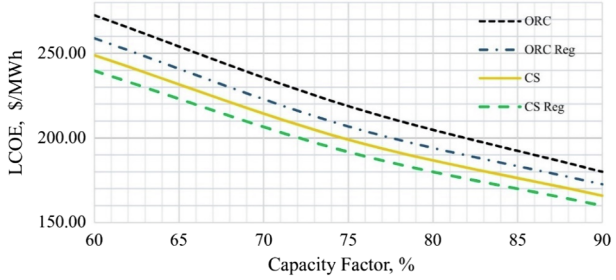

Fig. 9. LCOE of four investigated schemes as a function of CF.

In Table 8, the LCOE and system efficiency values are presented among other parameters of the LCOE-optimized results. System efficiency is expectedly lower than in case of the efficiency-optimization. Interestingly, CS Reg system shows the best LCOE, having the system efficiency practically equal to the CS one. For ORS systems, the relation of LCOE and η_{sys} is not the same: the scheme with higher efficiency (ORC Reg) has better LCOE value. More than that, the ORC Reg scheme has LCOE minimum with the parameters close to the efficiency-optimal ones; the efficiency is 0.36 absolute percent lower, whereas the efficiency of CS Reg lower at 1.4%, having a decrease from 12.49% to 11.09%. These variations are connected with the balance between sizes of heat exchangers; hence, their costs and power production of the system. The values of pinches of heat exchangers, which implicitly connected with size: smaller pinch gives larger HE, are presented in Table 8. It can be noticed that all schemes besides the ORC Reg have higher values of pinches than in the maximum efficiency case; this also correlates with the scheme efficiency trend itself. Other parameters presented in Table 8 gives more details of the system operation, enabling to reproduce or compare the results.

Table 8
Parameters of schemes LCOE-optimized for 90% CF.

Parameter	ORC	ORC Reg	CS	CS Reg
LCOE, $/MWt	181.0	169.8	166.0	159.5
Cap.cost, $/kW	1215	1140	1115	1065
P_{gross}, kW	141.3	154.1	152.8	152.9
P_{net}, kW	118.2	132.9	134.7	134.8
η_{sys}, %	9.73	10.94	11.08	11.09
π^*_T	n/a	n/a	2.87	2.90
P_T, kW	n/a	n/a	281.2	282.7
π_C	n/a	n/a	3.07	3.09
P_C, kW	n/a	n/a	213.6	215.2
$r_{v.Exp}$	46.4	35.1	44.3	39.8
P_{Exp}, kW	141.3	154.1	85.2	85.4
$P_{Pump.ORC}$, kW	6.61	6.32	3.96	3.92
$p_{Con.out}$, kPa	75.8	78.0	76.2	77.3
$p_{Pump.out}$, kPa	2700	2687	2687	2687
$\dot{m}_{w.f.}$, kg/s	1.25	1.10	0.75	0.74
$\dot{m}_{oil}$, kg/s	1.08	1.20	0.97	0.96
T_{cond}, °C	28.0	28.5	28.0	28.3
T_{evap}, °C	181.9	181.9	181.9	181.9
$T_{Exp.out}$, °C	101.4	145.0	101.7	110.2
$T_{Con.in}$, °C	101.4	59.8	101.7	71.6
$T_{s.h.}$, °C	5	40	6.3	11.2
$T_{exh.g.out}$, °C	78.0	144.5	189.8	166.1
Δ_{Ev}, °C	19.6	16.6	30.6	29.2
UA_{Ev}, kJ/(K × s)	10.81	10.83	10.03	10.89
Δ_{Con}, °C	5	5	5	5
UA_{Con}, kJ/(K × s)	78.06	70.83	46.9	44.72
Δ_{Regen}, °C	n/a	30.92	n/a	44.1
UA_{Regen}, kJ/(K × s)	n/a	5.33	n/a	1.22
$\Delta_{HE\text{-}1}$, °C	30	30	30	30
UA_{HE-1}, kJ/(K × s)	12.7	10.08	10.89	10.28
Δ_{Cooler}, °C	n/a	n/a	15	15
UA_{Cooler}, kJ/(K × s)	n/a	n/a	3.1	3.31

exhaust temperature reaches 600 °C. The suggested combined scheme was studied in two configurations: with regenerative ORC (CS Reg), and without regeneration (CS), for the number of temperatures in the range 470–570 °C with the temperature considered as nominal equal to 520 °C. As a benchmark for these schemes, a conventional ORC was considered, also in two configurations: regenerative (ORC Reg) and non-regenerative (ORC). The comparison of three common ORC working fluids of different critical temperature levels: R-245fa, pentane, and toluene, has shown pentane as a better working fluid for the studied nominal case. Pentane has demonstrated an advantage in the system efficiency under limitations adopted from literature, which enable to consider not only thermodynamics but the technical aspect as well. The outcome of the work is the comparison of all above-mentioned schemes after optimization of their system efficiency and after LCOE-based (levelized cost of energy) optimization. The sensitivity of the results to the applied assumptions has been checked. Besides, the analysis IBC has revealed a remarkable two-extremum dependence of generated power from the pressure ratio caused by water condensation occurring before the IBC compressor.

Efficiency optimization has shown around 10% advantage of CS Reg over the ORC Reg with absolute values equal to 12.49% and 11.3% correspondingly. This relative difference grows with the increase of turbine inlet temperature. In the same time, the comparison of the LCOE-optimized scheme also demonstrates the 6.4% (for capacity factor equals 0.9) advantage of CS Reg scheme but on the lower level of efficiency (11.09% for CS Reg versus 10.94% for ORC Reg). The obtained value of LCOE for CS Reg equals 159.5 $/MWh versus 169.8 $/MWh for ORC Reg. That can be explained by the major role of heat exchangers in the capital cost formation in comparison with the cost of machines. Note that the sensitivity analysis has shown that obtained values are considerably affected by the parameters of components, especially, by efficiencies of turbomachinery, which may considerably affect the performance of both systems. However, the outcomes of the

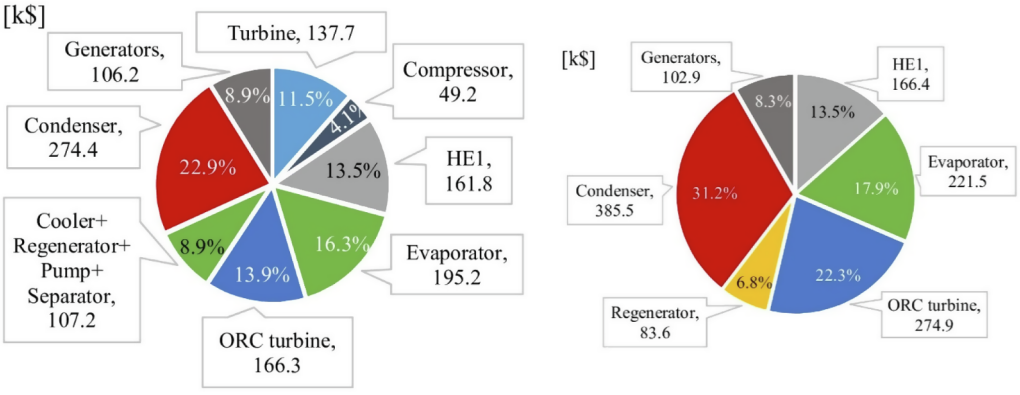

Fig. 10. Capital cost distribution between system components for CS Reg (left) and ORC Reg (right) optimized for CF = 90%.

4. Conclusion

This study investigated a combined inverted Brayton plus organic Rankine cycle (IBC-ORC), which, to the best of authors' knowledge, has never been studied. As a bright example, heavy-duty internal combustion engines may be mentioned as, up to certain capacity, their nominal scheme assessment are favorable enough to give room for further research of this technology.

Declaration of Competing Interest

None.

Acknowledgments

Kirill A. Abrosimov gratefully acknowledges Prof. Henni Ouerdane for careful reading of the manuscript, Prof. Federico Ibanez for technical consultation, Mikhail Pugach, Arseniy Sleptsov, Alexander Ryzhov, and Ekaterina Masloboeva for scientific discussions. Also, we extend our deep gratitude to Mike Bowman and Vitali Lissianski (GE Global Research, US) for insightful consultations.

Appendix A Chemical composition of the exhaust gas

With an assumption of the clean natural gas (e.g., Urengoy gas field) of a mass fraction of methane above 98% [62], the composition of the exhaust gas obtained in the combustion for the excess air ratio α = 1.2 and 60% air relative humidity is presented in Table A.1:

Table A.1
Exhaust gas composition.

Compound:	N_2	CO_2	H_2O	O_2	Ar
Mass fraction:	71.44%	12.59%	11.11%	3.65%	1.2%

Appendix B Basic equations of components

The power output from the Turbine and Expander was computed as:

$$P_T = \dot{m}_g \times (\mathrm{H}_{T.in} - \mathrm{H}_{T.out.is}) \times \eta_T \times \eta_{gen} \tag{B1}$$

$$P_{Exp} = \dot{m}_{w.f.} \times (\mathrm{H}_{Exp.in} - \mathrm{H}_{Exp.out.is}) \times \eta_{Exp} \times \eta_{gen} \tag{B2}$$

The power consumption of the Compressor was computed as:

$$P_C = \dot{m}_g \times (\mathrm{H}_{C.in} - \mathrm{H}_{C.out.is}) \times \frac{\eta_{gen}}{\eta_C} \tag{B3}$$

The power consumption of pumps was computed as:

$$P_{pump} = \frac{\dot{m}_{fluid} \times (\mathrm{p}_{pump.in} - p_{pump.out})}{\rho_{fluid} \times \eta_{pump}} \tag{B4}$$

η_T, η_{Exp}, η_C, η_{pump} are the isentropic (adiabatic) efficiency of the component.

The heat exchangers are simulated based on the “Simple weighted model” with about 30 intervals of equal enthalpy step with the following equation for each interval:

$$\dot{q}_{HE} = \dot{m}_{w.f.} \times (\mathrm{H}_{HE.i+1} - \mathrm{H}_{HE.i}) \tag{B5}$$

Appendix C Efficiency of turbomachines

The formula for the dependence between the efficiency of turbomachines in BC and IBC is derived in the following manner:

- $\frac{\rho_1}{\rho_2} = \frac{p_2}{p_1}$ – for the ideal gas at equal temperature.

where ρ – density (kg/m^3), p – pressure (Pa).

- Now BC and IBC turbomachines are compared with assumptions of equal inverse pressure ratio $\pi'_T = \frac{p_{T.in}}{p_{T.out}}$ above (BC) and below (IBC) atmospheric pressure and equal gas flow rate.

$$\frac{\rho_{IBC.out}}{\rho_{BC.out}} = \frac{p_{IBC.out}}{p_{BC.out}} = \frac{p_a/\pi'_T}{p_a} = \frac{1}{\pi'_T} \tag{C1}$$

- $S_{IBC} \times \rho_{IBC} \times v_{IBC} = S_{BC} \times \rho_{BC} \times v_{BC}$ - for a turbomachine of BC and IBC scheme with equal mass flow rate. Where S – square of the cross-section (m^2), v - the mean flow velocity (m/s).
- For equal velocities of the flow: $\frac{S_{IBC}}{S_{BC}} = \frac{\rho_{BC}}{\rho_{IBC}}$
- $S = f(D'^2)$ – for round-shape cross-sections of turbo-machines, where D’ - characteristic dimension (diameter). Considering Eq. (C.1):

$$\frac{D'_{IBC}}{D'_{BC}} = \sqrt{\frac{S_{IBC}}{S_{BC}}} = \sqrt{\frac{\rho_{BC}}{\rho_{IBC}}} = \sqrt{\pi'_T} \tag{C2}$$

- $Re = \frac{v \times D' \times \rho}{\mu}$ - Reynolds number, where μ – dynamic viscosity (Pa·s). μ – may be considered as independent from pressure in the considered range of pressures and temperatures (Kadoya (1985) [63]).
- From the definition of Reynolds number and Eqs. (C.1) and (C.2):

$$\frac{Re_{IBC}}{Re_{BC}} = \frac{v_{IBC} \times D'_{IBC} \times \rho_{IBC}}{\mu_{IBC}} / \frac{v_{BC} \times D'_{BC} \times \rho_{BC}}{\mu_{BC}} = \frac{D'_{IBC} \times \rho_{IBC}}{D'_{BC} \times \rho_{BC}} = \frac{\sqrt{\pi'_T}}{\pi'_T} = \frac{1}{\sqrt{\pi'_T}} \quad \text{(C3)}$$

- According to Henke (2013) [35], the following correlation can be observed:

$$\frac{1-\eta_1}{1-\eta_2} = \left(\frac{Re_2}{Re_1}\right)^n \quad \text{(C4)}$$

where

n	Re
0.06	1.21×10^6–3.03×10^6
0.09	0.43×10^6–1.21×10^6
0.2	0.34×10^6–0.43×10^6

According to the preliminary calculations, for this case, *Re* lays in the second range. However, n = 0.2 was used to avoid overestimation of the performance of the scheme.

- Combining Eqs. (C.3) and (C.4) the following results are obtained:

$$\eta_{IBC} = 1 - \pi'^{0.1}_T \times (1 - \eta_{BC}) \quad \text{(C5)}$$

Appendix D Description of the cost-functions

The equipment cost for different types of equipment according to applied MCT (Turton (2008) [47]) is considered either in the way of purchase cost with several factors or only bare module cost. The purchase cost may be defined as:

$$C_{BM} = C_{b.c.} \times F_{BM} \quad \text{(D.1)}$$

where the $C_{b.c.}$ – "base conditions" cost calculated as:

$$\lg(C_{b.c.}) = K_1 + K_1 \times \lg(A) + K_1 \times (\lg(A))^2 \quad \text{(D.2)}$$

and A is a capacity or size parameter of equipment, F_{BM} – bare module factor equals to:

$$F_{BM} = B_1 + B_2 \times F_P \times F_M \quad \text{(D.3)}$$

where FM – "material factor" peculiar for each material different from the basic one; F_P – "pressure factor" equals to:

$$\lg(F_P) = C_1 + C_1 \times \lg(p) + C_1 \times (\lg(p))^2 \quad \text{(D.4)}$$

For some equipment, the bare module factor is given, and the bare module equipment cost should be calculated with the Eq. (D.1).

To calculate total module cost which conceder mounting and axillary devices including TOL, the following formula from Turton (2008) [47] is applied:

$$C_{TM} = 1.18 \times C_{BM} \quad \text{(D.5)}$$

Table D.1 presents all applied coefficient and alternative equations been used in some cases.

Table D.1
Coefficients for the components cost-functions.

Component	Function argument	K_1 K_2 K_3	B_1 B_2	F_M	C_1 C_2 C_3	F_{BM}
IBC Turbine ● Turton (2008) [47]: radial turbine ● $ 2001	P (kW)	2.2476 1.4965 −0.1618	– –	–	– – –	3.5
ORC expander ● Turton (2008) [47]: radial turbine ● $ 2001	P (kW)	2.2476 1.4965 –0.1618	– –	–	– – –	3.5
Compressor ● Calise (2007) [76]: radial compressor ● € 2003	P (kW)	$C_{BM} = 91562 \times (P_{Comp}/445)\hat{}0.67$				–
HE-1 ● Turton (2008) [47]: fixed tube ● $ 2001	A (m^2)	4.3247 –0.303 0.1634	1.63 1.66	1.81	$F_p = 1.25$	–
Condenser ● Lemmens (2016) [56] ● $ 2000	Heat flow (kW)	$C_{b.c.} = 12300 \times \left(\frac{P_{HE.heat}}{50}\right)^{0.76}$	0.96 1.21	1.81	$F_p = 1.25$	–

(*continued on next page*)

Table D.1 (*continued*)

Component	Function argument	K_1 K_2 K_3	B_1 B_2	F_M	C_1 C_2 C_3	F_{BM}
Evaporator ● Turton (2008) [47]: bayonet ● $ 2001	A (m^2)	4.2768 –0.0495 0.1431	1.63 1.66	1.81	0.03881 –0.11272 0.08183	–
Cooler ● Turton (2008) [47]: air cooled ● $ 2001	A (m^2)	2.7652 0.7282 0.0783	1.74 1.55	1.81	$F_p = 1.25$	–
ORC pump ● Turton (2008) [47]: centrifugal pump ● $ 2001	P (kW)	3.3892 0.0536 0.1538	1.89 1.35	1.6	–0.3935 0.3957 –0.00226	–
Oil pump ● Turton (2008) [47]: centrifugal pump ● $ 2001	P (kW)	3.3892 0.0536 0.1538	1.89 1.35	1.6	–0.3935 0.3957 –0.00226	–
Regenerator ● Turton (2008) [47]: air cooled ● $ 2001	A (m^2)	2.7652 0.7282 0.0783	1.74 1.55	1.81	$F_p = 1.25$ (for subatmospheric conditions)	
Electrical generator ● Lemmens (2016) [56] ● € 1993	P (kW)		$C_p = 1850000 \times (P/11800)^{0.94}$ Power factor[1] = 1.2			1.5
Separator ● Garrett (2012) [57] ● $ 1997	$\dot{m}$ (m^3/h)	Constant value based on the type of separator, volumetric flow rate and material (equal to 23.0 k$)				

[1] Power factor stands for the additional capacity of a generator above the nominal value of the prime mover power

References

[1] The Paris Agreement|UNFCCC < https://unfccc.int/process/the-paris-agreement/what-is-the-paris-agreement/ > ; n.d. [accessed January 9, 2019].

[2] 2010 to 2015 government policy: energy demand reduction in industry, business and the public sector - GOV.UK, < https://www.gov.uk/government/publications/2010-to-2015-government-policy-energy-demand-reduction-in-industry-business-and-the-public-sector/2010-to-2015-government-policy-energy-demand-reduction-in-industry-business-and-the-public-sector#appendix-4-clima/ > ; n.d. [accessed January 9, 2019].

[3] Federal Energy Management Program|Department of Energy, < https://www.energy.gov/eere/femp/federal-energy-management-program/ > ; n.d. [accessed January 9, 2019].

[4] Jouhara H, Khordehgah N, Almahmoud S, Delpech B, Chauhan A, Tassou SA. Waste heat recovery technologies and applications. Therm Sci Eng Prog 2018;6:268–89. https://doi.org/10.1016/J.TSEP.2018.04.017.

[5] Lecompte S, Henk H, van den Broek M, Bruno V, Michel DP. Review of organic Rankine cycle (ORC) architectures for waste heat recovery. Renew Sustain Energy Rev 2015;47:448–61. https://doi.org/10.1016/j.rser.2015.03.089.

[6] Lion S, Michos CN, Vlaskos I, Rouaud C, Taccani R. A review of waste heat recovery and Organic Rankine Cycles (ORC) in on-off highway vehicle Heavy Duty Diesel Engine applications. Renew Sustain Energy Rev 2017;79:691–708. https://doi.org/10.1016/J.RSER.2017.05.082.

[7] Campana F, Bianchi M, Branchini L, De Pascale A, Peretto A, Baresi M, et al. ORC waste heat recovery in European energy intensive industries: energy and GHG savings. Energy Convers Manage 2013;76:244–52. https://doi.org/10.1016/J.ENCONMAN.2013.07.041.

[8] Wang X, Dai Y. Exergoeconomic analysis of utilizing the transcritical CO2 cycle and the ORC for a recompression supercritical CO2 cycle waste heat recovery: a comparative study. Appl Energy 2016;170:193–207. https://doi.org/10.1016/J.APENERGY.2016.02.112.

[9] Marchionni M, Bianchi G, Tassou SA. Techno-economic assessment of Joule-Brayton cycle architectures for heat to power conversion from high-grade heat sources using CO2 in the supercritical state. Energy 2018;148:1140–52. https://doi.org/10.1016/J.ENERGY.2018.02.005.

[10] Yari M, Mehr AS, Zare V, Mahmoudi SMS, Rosen MA. Exergoeconomic comparison of TLC (trilateral Rankine cycle), ORC (organic Rankine cycle) and Kalina cycle using a low grade heat source. Energy 2015;83:712–22. https://doi.org/10.1016/J.ENERGY.2015.02.080.

[11] Fischer J. Comparison of trilateral cycles and organic Rankine cycles. Energy 2011;36:6208–19. https://doi.org/10.1016/J.ENERGY.2011.07.041.

[12] Nemati A, Nami H, Ranjbar F, Yari M. A comparative thermodynamic analysis of ORC and Kalina cycles for waste heat recovery: a case study for CGAM cogeneration system. Case Stud Therm Eng 2017;9:1–13. https://doi.org/10.1016/J.CSITE.2016.11.003.

[13] Bianchi M, De Pascale A. Bottoming cycles for electric energy generation: parametric investigation of available and innovative solutions for the exploitation of low and medium temperature heat sources. Appl Energy 2011;88:1500–9. https://doi.org/10.1016/J.APENERGY.2010.11.013.

[14] Nader WB, Mansour C, Dumand C, Nemer M. Brayton cycles as waste heat recovery systems on series hybrid electric vehicles. Energy Convers Manage 2018. https://doi.org/10.1016/j.enconman.2018.05.004.

[15] Lee HY, Park SH, Kim KH. Comparative analysis of thermodynamic performance and optimization of organic flash cycle (OFC) and organic Rankine cycle (ORC). Appl Therm Eng 2016;100:680–90. https://doi.org/10.1016/J.APPLTHERMALENG.2016.01.158.

[16] Baccioli A, Antonelli M, Desideri U. Technical and economic analysis of organic flash regenerative cycles (OFRCs) for low temperature waste heat recovery. Appl Energy 2017;199:69–87. https://doi.org/10.1016/j.apenergy.2017.04.058.

[17] Wang K, Sanders SR, Dubey S, Choo FH, Duan F. Stirling cycle engines for recovering low and moderate temperature heat: a review. Renew Sustain Energy Rev 2016;62:89–108. https://doi.org/10.1016/J.RSER.2016.04.031.

[18] Zhang Y, Cleary M, Wang X, Kempf N, Schoensee L, Yang J, et al. High-temperature and high-power-density nanostructured thermoelectric generator for automotive waste heat recovery. Energy Convers Manage 2015;105:946–50. https://doi.org/10.1016/J.ENCONMAN.2015.08.051.

[19] Zhai H, An Q, Shi L, Lemort V, Quoilin S. Categorization and analysis of heat sources for organic Rankine cycle systems. Renew Sustain Energy Rev 2016;64:790–805. https://doi.org/10.1016/J.RSER.2016.06.076.

[20] Shi L, Shu G, Tian H, Deng S. A review of modified Organic Rankine cycles (ORCs) for internal combustion engine waste heat recovery (ICE-WHR). Renew Sustain Energy Rev 2018;92:95–110. https://doi.org/10.1016/J.RSER.2018.04.023.

[21] Therminol VP-1 < https://www.therminol.com/sites/therminol-prd.us-east-1.elasticbeanstalk.com/files/documents/TF09A_Therminol_VP1.pdf/ > ; n.d. [accessed January 9, 2019].

[22] Thekdi Arvind NS. Industrial Waste Heat Recovery: Potential Applications, Available Technologies and Crosscutting R&D Opportunities. 2014. DOI:10.2172/1185778.

[23] The World Factbook — Central Intelligence Agency < https://www.cia.gov/library/publications/resources/the-world-factbook/rankorder/2233rank.html/ > ; n.d. [accessed December 27, 2018].

[24] Technical Downloads|GE Power Generation < https://www.ge.com/power/resources/downloads/ > ; n.d. [accessed January 9, 2019].

[25] Cat|Oil and Gas|Caterpillar < https://www.cat.com/en_US/products/new/power-systems/oil-and-gas/ > ; n.d. [accessed January 9, 2019].

[26] Elfasakhany A. Performance and emissions analysis on using acetone–gasoline fuel blends in spark-ignition engine. Eng Sci Technol Int J 2016;19:1224–32. https://doi.org/10.1016/J.JESTCH.2016.02.002.

[27] Masum BM, Kalam MA, Masjuki HH, Palash SM, Fattah IMR. Performance and emission analysis of a multi cylinder gasoline engine operating at different alcohol–gasoline blends. RSC Adv 2014;4:27898–904. https://doi.org/10.1039/C4RA04580G.

[28] Zeb K, Ali SM, Khan B, Mehmood CA, Tareen N, Din W, et al. A survey on waste heat recovery: electric power generation and potential prospects within Pakistan. Renew Sustain Energy Rev 2017;75:1142–55. https://doi.org/10.1016/J.RSER.2016.11.

096.
[29] Bianchi M, Negri di Montenegro G, Peretto A, Spina PR. A feasibility study of inverted brayton cycle for gas turbine repowering. J Eng Gas Turbines Power 2005;127:599. https://doi.org/10.1115/1.1765121.
[30] Shabana N. QATAR NATIONAL CEMENT COMPANY Cement Rotary Kiln Questions and Answers; 2013.
[31] Neeharika Naik-Dhungen. WASTE HEAT TO POWER SYSTEMS; 2012.
[32] Sprouse C, Depcik C. Review of organic Rankine cycles for internal combustion engine exhaust waste heat recovery. Appl Therm Eng 2013;51:711–22. https://doi.org/10.1016/J.APPLTHERMALENG.2012.10.017.
[33] Yue C, Han D, Pu W. Analysis of the integrated characteristics of the CPS (combined power system) of a bottoming organic Rankine cycle and a diesel engine. Energy 2014;72:739–51. https://doi.org/10.1016/J.ENERGY.2014.05.103.
[34] Xu B, Rathod D, Yebi A, Filipi Z, Onori S, Hoffman M. A comprehensive review of organic rankine cycle waste heat recovery systems in heavy-duty diesel engine applications. Renew Sustain Energy Rev 2019;107:145–70. https://doi.org/10.1016/J.RSER.2019.03.012.
[35] Henke M, Monz T, Aigner M. Inverted Brayton cycle with exhaust gas recirculation—a numerical investigation. J Eng Gas Turbines Power 2013;135:091203https://doi.org/10.1115/1.4024954.
[36] Agelidou E, Monz T, Huber A, Aigner M. Experimental investigation of an inverted Brayton Cycle micro gas turbine for CHP application. Microturbines, Turbochargers Small Turbomachines; Steam Turbines, vol. 8. ASME; 2017. https://doi.org/10.1115/GT2017-64490. p. V008T26A023.
[37] Valdés M, Abbas R, Rovira A, Martín-Aragón J. Thermal efficiency of direct, inverse and sCO2 gas turbine cycles intended for small power plants. Energy 2016;100:66–72. https://doi.org/10.1016/j.energy.2016.01.072.
[38] Venkata Rao R, Patel V. Multi-objective optimization of combined Brayton and inverse Brayton cycles using advanced optimization algorithms. Eng Optim 2012;44:965–83. https://doi.org/10.1080/0305215X.2011.624183.
[39] Matviienko V, Ocheretianyi V, Andriets O, Riznyk S. Working process control in a ship gas turbine engine of complex cycle. Aircr. Engine; Fans Blowers; Mar. vol. 1. ASME; 2016. https://doi.org/10.1115/GT2016-56073. p. V001T22A001.
[40] Ceen B, Jones S, Chen Z, Agurto Goya A, Copeland C. Modeling and simulation of an inverted Brayton cycle as an exhaust-gas heat-recovery system. J Eng Gas Turbines Power 2017. https://doi.org/10.1115/1.4035738.
[41] Hu B, Akehurst S, Brace C. Novel approaches to improve the gas exchange process of downsized turbocharged spark-ignition engines: a review. Int J Engine Res 2016;17:595–618. https://doi.org/10.1177/1468087415599866.
[42] Weber J, Straub D. Inverted Brayton cycle for use with chemical looping combustion. 8th Annu Int. Energy Convers. Eng. Conf. Reston, Virigina: American Institute of Aeronautics and Astronautics; 2010. https://doi.org/10.2514/6.2010-6606.
[43] Patent Search Software - IP Search Services - IP.com < https://ip.com/ > ; n.d.
[44] Quoilin S, Declaye S, Legros A, Guillaume L, Lemort V. Working fluid selection and operating maps for Organic Rankine Cycle expansion machines. 21st Int Compress. Conf. Purdue. 2012. p. 10.
[45] Abrosimov KA, Galkin DI, Tumashev RZ, Ustinov AA. Simulation of CHP system based on micro gas turbine with inverted Brayton cycle. Coal, Biomass Altern. Fuels; Cycle Innov. Electr. Power; Ind. Cogener. Appl. Org. Rank. Cycle Power Syst. vol. 3. ASME; 2017. https://doi.org/10.1115/GT2017-64029. p. V003T06A019.
[46] Ferguson CR, Kirkpatrick A. Internal combustion engines: applied thermosciences. n.d.
[47] Turton R, Bailie RC, Whiting WB, Shaeiwitz JA. Analysis, synthesis and design of chemical processes. In: Turton Richard, Bailie Richard C, Whiting Wallace B, Joseph A, editors. Shaeiwitz - Google Книги. 3rd ed.Pearson Education; 2008. doi:10.978.013245/9181.
[48] Dixon SL, Hall CA. Fluid mechanics and thermodynamics of turbomachinery. 6th ed. Butterworth-Heinemann is an imprint of Elsevier; 2010.
[49] Sinnott RK, Coulson JM, Coulson and Richardson's chemical engineering. In: Chemical engineering design. 4th ed. vol. 6. Elsevier Butterworth-Heinemann; 2005. DOI:10.978.075066/5384.
[50] Antonelli M, Baccioli A, Francesconi M, Desideri U. Dynamic modelling of a low-concentration solar power plant: a control strategy to improve flexibility. Renew Energy 2016;95:574–85. https://doi.org/10.1016/j.renene.2016.04.053.
[51] Baccioli A, Antonelli M, Desideri U, Grossi A. Thermodynamic and economic analysis of the integration of Organic Rankine Cycle and Multi-Effect Distillation in waste-heat recovery applications. Energy 2018;161:456–69. https://doi.org/10.1016/j.energy.2018.07.150.
[52] Pili R, Romagnoli A, Spliethoff H, Wieland C. Techno-economic analysis of waste heat recovery with ORC from fluctuating industrial sources. Energy Procedia 2017;129:503–10. https://doi.org/10.1016/J.EGYPRO.2017.09.170.
[53] Freyman T, Tran T. Renewable energy discount rate survey results-2018. UK: 2019. < https://www.grantthornton.co.uk/globalassets/1.-member-firms/united-kingdom/pdf/documents/renewable-energy-discount-rate-survey-results-2018.pdf > .
[54] Toffolo A, Lazzaretto A, Manente G, Paci M. A multi-criteria approach for the optimal selection of working fluid and design parameters in Organic Rankine Cycle systems. Appl Energy 2014;121:219–32. https://doi.org/10.1016/J.APENERGY.2014.01.089.
[55] Smith R. Chemical process design and integration. John Wiley & Sons; 2005.
[56] Lemmens S. Cost, engineering techniques and their applicability for cost estimation of organic rankine cycle systems. Energies 2016;9:485. https://doi.org/10.3390/en9070485.
[57] Garrett DE. Chemical engineering economics Van Nostrand Reinhold; 2012. https://doi.org/10.1007/9789401165440.
[58] Chemical Engineering - Chemical Engineering essentials for the global chemical processing industries (CPI), < https://www.chemengonline.com/ > ; 2019 [accessed December 28, 2018].
[59] Free Online Exchange Rates Conversion Calculator, < https://freecurrencyrates.com/ > ; 2019 [accessed January 9, 2019].
[60] Delgado-Torres AM, García-Rodríguez L. Preliminary assessment of solar organic Rankine cycles for driving a desalination system. Desalination 2007;216:252–75. https://doi.org/10.1016/j.desal.2006.12.011.
[61] Kennedy I, Chen Z, Ceen B, Jones S, Copeland CD. Inverted Brayton cycle with exhaust gas condensation. Microturbines, Turbochargers Small Turbomachines; Steam Turbines, vol. 8. ASME; 2017. https://doi.org/10.1115/GT2017-64695. p. V008T26A026.
[62] Grace JD, Hart GF. Giant gas fields of Northern West Siberia. Am Assoc Pet Geol Bull 1986;70:23. https://doi.org/10.1306/94886358-1704-11D7-8645000102C1865D.
[63] Kadoya K, Matsunaga N, Nagashima A. Viscosity and thermal conductivity of dry air in the gaseous phase. J Phys Chem Ref Data 1985;14:947–70. https://doi.org/10.1063/1.555744.